IJMPR 2022, 6(10), 01-17

International Journal of Modern Pharmaceutical Research
www.ijmpronline.com

ISSN: 2319-5878
IJMPR
Research Article
SJIF Impact Factor: 5.273

ENHANCEMENT OF RESVERATROL DISSOLUTION VIA CO-GRINDING TECHNIQUE: DEVELOPMENT AND EVALUATION OF BUCCAL FILM

Ayatallah A. Taelab*[1], Heba I. Elagamy[1] and Ebtessam A. Essa[2]

[1]Department of Pharmaceutical Technology, Faculty of Pharmacy, Delta University for Science and Technology, Egypt.
[2]Department of Pharmaceutical Technology, Faculty of Pharmacy, Tanta University, Egypt.

Received on: 15/09/2022
Revised on: 05/10/2022
Accepted on: 25/10/2022

***Corresponding Author**
Ayatallah A. Taelab
Department of Pharmaceutical Technology, Faculty of Pharmacy, Delta University for Science and Technology, Egypt.

ABSTRACT

Trans-resveratrol (RES), among other antioxidants, has recently gained considerable scientific attention due to its protective action against oxidative stress Oromucosal delivery fulfills the urge for more patient compliance, especially the elderly, by formulating convenient dosage forms. Additionally, improved bioavailability is expected due to avoidance of presystemic metabolism of RES. The aim of the present study was to improve the dissolution of RES via modification of its crystalline packing utilizing ethanol- assisted co-grinding with either ascorbic acid (AA) or L-arginine (L-Ar) at 1:1, 1:2, 1:3 molar ratios and prepare fast dissolving buccal films. The composites were evaluated using FTIR, DSC, XRD, and in vitro dissolution. The antioxidant activity of RES after processing was evaluated. Rapid disintegrating buccal films were prepared by casting technique using hydroxypropyl methylcellulose and polyvinylpyrrolidone as film-forming polymers. Physical characterization suggested modulation of RES crystalline nature with possible formation of new species, probably co-crystals. Both excipients improved RES, with L-Ar being superior to AA. The prepared composites preserved the antioxidant activity of RES. The optimized formulations F3 (RES: AA at 1:3) and F5 (RES: L-Ar at 1:2) were successively incorporated in fast disintegrating oral films with prompt RES release of 89.0 and 80.0% after 5 minutes, respectively. The results indicated that treating RES with either AA or L-Ar was a useful tool to improve dissolution. Additionally, rapidly disintegrating buccal film is expected to improve RES bioavailability by avoiding its pre-systemic degradation.

KEYWORDS: Resveratrol, ascorbic acid, arginine, oral film, buccal film.

Graphical abstract

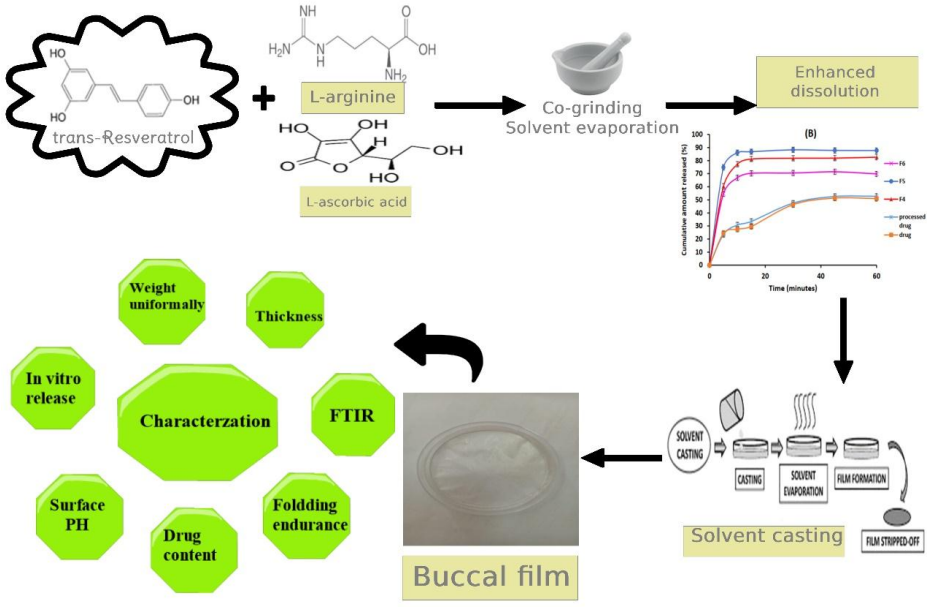

INTRODUCTION

Trans-resveratrol (RES) is a nutraceutical that belongs to a group of compounds known as polyphenol that relates to the stilbene family (3,4',5-trihydroxy-trans-stilbene). RES consists of two phenolic rings linked together via ethylene bridge (Figure 1). It is present in many plants like grapes, berries, peanuts and other vegetables. RES has recently gained considerable scientific attention due to its biological significance and disease-fighting qualities that arise from its protective action against oxidative stress (Marques et al., 2009; Risuleo, 2016).

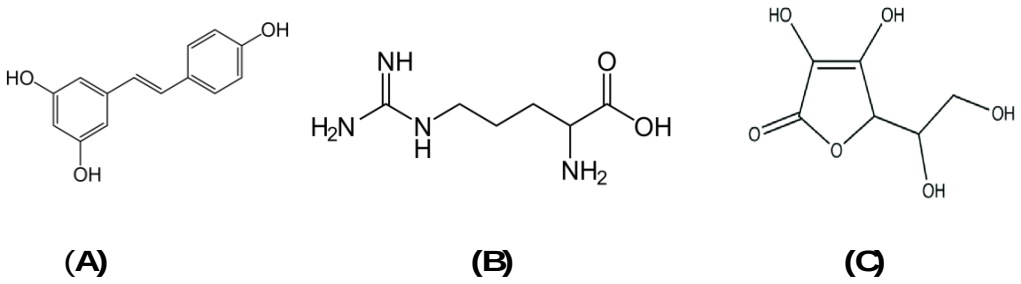

(A) **(B)** **(C)**

Figure 1: Chemical structure of resveratrol and the used additives where (A) is for resveratrol (B) is for arginine and (C) is for ascorbic acid.

Unfortunately, the polyphenolic structure of RES imparts a hydrophobic nature to the compound making it practically insoluble in water (log P of 3.1) (Kristl et al., 2009). This, together with extensive hepatic first pass metabolism, limits its oral bioavailability (Kapetanovic et al., 2011). In order to obtain the utmost benefit of RES following oral administration, many studies were conducted to increase its dissolution rate with promising results. These trials included formation of solid dispersion (Ha et al., 2021), composite nanoparticles (Ha et al., 2019), self-emulsifying drug delivery (Balata et al., 2016), nanosuspension (Hao et al., 2015) among others.

Most approaches involved the use of sophisticated techniques and/or equipment. Recently, a more economic and scalable technique that is largely investigated among pharmaceutical formulators is the modulation of the crystalline structure of the active pharmaceutical ingredient (API). This is the use of simple co-grinding technique employing benign guest molecule. This modulation usually results in considerable improvement in the aqueous solubility of hydrophobic drugs due to modification of molecular packing characteristics in the crystal lattice of the API. Based on the physicochemical properties of both API and guest molecule, the latter can act as a co-former for the newly formed solid crystalline species which could be co-crystal, eutectic, solvate, co-amorphous or salt (Essa et al., 2019; Elshaikh et al., 2019; Elkholy et al., 2020; Karagianni et al. 2018; Weyna et al. 2012; Naem et al., 2020). The work to improve RES delivery via optimization of its solid-state characteristics is scarce. In one study, RES was used as co-crystal co-former and not as API (Kavuru et al., 2010). As per three hydrogen groups (Figure1), RES is promising in formation of co-crystal when using the suitable co-former. Zhou and coworkers prepared RES co-crystal using isoniazide and 5-aminobenzamide as co-former with promising results (Zhou et al., 2016).

This study was conducted to improve RES aqueous solubility by liquid assisted co-grinding technique with the aim of preparing fast dissolving buccal films. The urge for more patient compliance to medication, especially for geriatric and pediatric population, had driven pharmaceutical formulators to focus on the more convenient drug delivery systems. Buccal cavity with its mucus membrane is an attractive site for convenient drug delivery.

To achieve this aim, RES was cogrinded with two different guest molecules. The selected guest molecules were part of our daily food intake that would, in addition to increase RES aqueous solubility, provide additional health benefits. These molecules were the organic acid Ascorbic acid (AA) and the amino acid L-arginine (L-Ar). AA, also known as vitamin C, which is a natural water-soluble vitamin with potent antioxidant activity that plays an important part in many physiological processes within the human body (Attia et al., 2020). AA was previously investigated as co-crystals co-former for other API with encouraging results (Nicolov et al., 2019; Kovac-Besovi´c et al., 2009; Meepripruk et al., 2016). Therefore, it was selected as a potential modulator to RES crystalline structure, Additionally, the antioxidant activity of RES is expected to be fortified by that of AA due to synergistic effect.

L-Ar was used because amino acids are one of the highly promising candidates as a guest molecule due to their functional groups that can form hydrogen bonds with different molecules. L-Ar was successively used as co-crystal conformer (Chi et al., 2013), with potential antioxidant activity (Abu-Serie et al., 2015; Shan et al., 2015).

MATERIALS AND METHODS

Materials

RES was purchased from Xian Lukee Bio-Tech Co., Ltd., (Xi'an, Shaanxi Sheng, People's Republic of

China). Ascorbic acid (AA) and L-arginine (L-Ar) were obtained as a gift sample from Sigma for Pharmaceutical Industries, Quesna, Egypt. Ethanol (pharmaceutical grade) was purchased from EL Nasr Pharmaceuticals Chemicals CO., Cairo, Egypt. Hydroxypropyl methyl cellulose (HPMC) E50 and polyvinylpyrrolidone K30 (PVP) were purchased from Loba Chemie, India.

UV Spectroscopic assay of resveratrol (RES)

Standard stock solution of RES (25µg/ml) was prepared by dissolving 25µg of RES in 25 ml of ethanol. Serial dilutions were prepared by diluting the stock solution with either distilled water or phosphate buffer pH value of 6.8. The absorbances of the prepared solutions were obtained at wavelength (λ) of 304 nm against blank using UV-spectrophotometer (Thermo Fisher Scientific, Evo300pc, USA). The calibration curve was constructed by plotting the absorbance as function of concentration. The obtained calibration curve was linear (R2=0.996) over the used concentrations range.

Preparation of co-grinded formulations

Table 1 shows the compositions of different formulations presented as molar ratio. Liquid assisted technique was adopted to prepare the co-grinded composite (Essa et al., 2019). Formulations F1, F2 and F3 were prepared by mixing 228mg of RES with 176.1, 352.2 or 528.4 mg of AA, respectively. Formulations F4, F5 and F6 were prepared by mixing 228 mg of RES with 174.2, 248.4 or 522.6 mg of L-Ar. Both RES and either AA or L-Ar were co-grinded using mortar and pestle with the drop wise addition of ethanol till obtaining a thin paste. The paste was subjected to continuous grinding till evaporation of the organic solvent and formation of dry powder. The powder was left overnight to ensure complete elimination of residual solvent. Pure RES, without additives, was similarly treated and was taken as a positive control.

Preparation of physical mixtures

Physical mixture (PM) of selected formulations (F3 and F5) were prepared. This was obtained by geometric dry blending of RES with either AA (PM1) or L-Ar (PM2) according to compositions in Table 1, with the aid of a mortar and a pestle.

Table 1: The composition of the prepared formulations presented as molar ratio.

Formulation	Resveratrol (mg)	Ascorbic (mg)	Arginine (mg)
Pure resveratrol	20		
F1	1	1	
F2	1	2	
F3	1	3	
F4	1		1
F5	1		2
F6	1		3
PM1	1	3	
PM2	1		2

Characterization of the prepared formulations

Fourier–transform infrared spectroscopy (FTIR)

The FTIR spectra of unprocessed RES, processed (wet grinded) RES (positive control), AA, L-Ar and their composites were recorded using a FTIR spectrophotometer (Bruker Tensor 27, Ettlingen, Germany). Samples were blended with potassium bromide (purified grade) prior to compression into thin disks. Tested samples were then scanned from 4000 to 400 cm^{-1}. The equipment employed a triglyceride sulphate (TGS) detector and is supported by Opus IR, FTIR software that was utilized in spectral data analysis.

Powder X-ray Diffraction (PXRD)

The crystalline structure of the of unprocessed RES, processed RES (positive control), AA, L-Ar and their formulations were examined using X-ray powder diffractometer (XRPD) (Bruker AXS GmbH, Karlsruhe, Germany) with Cu K λα radiation (λ= 1.5406 Å) and a VÅNTEC-1 detector. The data was collected at ambient temperature, with a 2θ scan axis. The scanning step size was set at 0.02^{o} and at a range of 5-60 ^{o} with 40-kV voltage.

Differential Scanning Calorimetry (DSC)

Thermal behavior of the unprocessed RES processed RES (positive control), AA, L-Ar and their co-grinded formulations were characterized using differential scanning calorimeter (DSC-60A, Shimadzu, Japan). The scanning was performed over a temperature range of 30 °C to 400 °C with a heating rate of 10 °C/min. The apparatus cell was first calibrated with high purity indium. Dry nitrogen was employed as the purging gas at a rate of 35 mL/min in all runs.

In vitro dissolution study of the prepared formulations

The *in vitro* dissolution of RES from the prepared formulations, processed (positive control) and unprocessed form was performed using USP Dissolution tester Apparatus II (Copley, NG 42JY, Nottingham, UK). Processed (wet grinded) and unprocessed RES were also tested and taken as positive and negative control, respectively. An amount equivalent to 20 mg of RES was

used. The dissolution medium was 900 mL distilled water maintained at 37°C±0.5°C and the paddle speed was adjusted to 100 rpm, similar to published data (Balata et al., 2016). 5 mL samples were withdrawn at specific intervals, filtered using membrane filter (0.45 µm Millipore filter). Samples were assayed spectrophotometrically at 304 nm for RES content. Equal volumes of distilled water were added to compensate for the withdrawn samples to keep constant volume. Dissolution profiles were constructed by drawing the cumulative amount of RES released as a function of time. This experiment was conducted in triplicate. The dissolution graphs were used to calculate the dissolution parameters to compare between different formulations. These parameters were the percentage amount released after 5 minutes and dissolution efficiency (DE). The dissolution efficiency is defined as the area under the dissolution plot up to certain time (t) expressed as its percentage relative to the area of the rectangle when complete (i.e.,100%) dissolution at the same time occurs (Khan, 1975).

Evaluation of the Antioxidant activity (AOA)

The antioxidant activity of unprocessed RES and selected formulations (F3 and F5) was determined employing 2,2-diphenyl-1-picrylhydrazyl (DPPH) free radical scavenging assay method (Nicolov et al., 2019; Rahman et al.,2015). The test is based on the change of the violet color of DPPH methanolic solution to shades of yellow color in presence of antioxidants.

Methanolic solution of DPPH (0.004%, w/v) was freshly prepared and stored at 10°C until used. This solution showed a dark violet color. Solutions of the investigated formulations and RES were prepared in methanol at various concentrations (5, 10, 20, 40, 80, 160, 320, 640 µg/ml).

Exactly measured 3 ml of DPPH was added to 40 ml of each tested solution and allowed to stand in the dark for 30 minutes at room temperature. Solution of ascorbic acid was used as reference compound. The absorbance was then recorded colorimetrically using UV-visible spectrophotometer at 517nm. The antioxidant activity (AOA), expressed as percentage, was determined by measuring the absorbance of the remaining DPPH radical as function of concentration using the following equation (Yen and Duh, 1994):

$PI = [(A_{control} - A_{test}) / A_{control}] \times 100\%$

where $A_{control}$ = absorbance of DPPH methanolic solution at time zero and A_{sample} is the absorbance of DPPH complex with RES after 30 min.

Preparation of rapidly dissolving buccal films

The optimized formulations of RES with either AA or L-Ar were formulated into buccal films. For comparison purposes, film containing unprocessed RES was also prepared. The films were assigned as Film 1, Film 2 and Film3 for those containing RES, F3 and F5, respectively. The composition of the prepared films is shown in Table 2. Solvent casting was employed in accordance with the previously published method with slight adjustment (Shimoda et al., 2009; Elagamy et al., 2019). PVP and HPMC were used as film-forming polymers. Both polymers were dissolved in 20 ml of ethanol/water (1:1 ratio) mixture under continuous agitation (100 rpm) using hot plate magnetic stirrer at 50°C. After cooling down, the selected formulation or unprocessed RES was added to the polymeric solution while stirring to achieve a uniform distribution. Finally, glycerol was added as a plasticizer at a concentration of 10% of the total film weight. Liquids were sonicated to get rid of entrapped air bubbles.

Each liquid was then poured into plastic petri dish having area of 22.1 cm^2. The plates were kept in an oven at 50°C until drying. The dried films were carefully scraped off and examined visually for any imperfections or entrapped air bubbles. To retain their integrity, the films were individually wrapped in aluminium foil and stored at room temperature in a desiccator until further use.

Evaluation of RES buccal films

Film weight

Prior to use, each film was cut, using scissor, into three square pieces each of 2×2 cm dimension. The weight of each film was measured using digital balance and average weight and standard deviation were recorded.

Table 2: Composition of the prepared fast dissolving resveratrol films, together with the quality control data and dissolution parameters.

	RES	F3	F5	HPMC	PVP	Glycerol	Dissolution Time (s)	Drug content (%)	Surface pH	Weight (mg)	Q5	DE (%)
Film1	110	-	-	200	100	45	72±2	102.5 ±1.2	5.7 ±0.1	75.5 ±1.7	52.3 ±1.3	40.1 ±0.1
Film2	-	151		200	100	50	45±1.5	94.8 ±0.1	5.9 ± 0.1	74.6 ± 2.0	89. 6 ±4.0	66.5 ±0.5
Film3	-	-	115	200	100	46	45±2.8	91.6 ±0.4	6.4 ±0.4	82.4 ±1.4	79.5 ±1.0	92.3 ±0.8

- Film 1, Film 2 and Film 3 were prepared using unprocessed resveratrol, formula F3 and formula F5, respectively
- Q5 amount of resveratrol dissolved after 5 minutes
- DE is dissolution efficiency expressed as percentage

Thickness
The thickness of each film was measured using micrometer. The measurements were recorded at five different positions of the same film and the average thickness was calculated.

Surface pH value
Each film (2x2 cm) was placed in a Petri dish and moistened by addition of 2ml phosphate buffer (pH 6.8), simulating the buccal media, and kept for 30 seconds. A pH meter electrode was used to measure the surface pH after being allowed to equilibrate for 1 minute. The experiment was repeated three times. The mean and standard deviation were then calculated (Elagamy et al., 2019; Brindle and Krochta, 2008).

Folding endurance
This test was performed to evaluate the ability of the film to withstand repeated folding and bending. Each film (2x2 cm) was subjected to repeated folding and the number of folding cycles needed to break the film was calculated (Elagamy et al., 2019; Brindle and Krochta, 2008).

Drug content
Drug content was evaluated by cutting three pieces (each 2x2 cm) of each film. Each piece was then dissolved in 100 ml of phosphate buffer (pH = 6.8), filtered and drug concentration was determined spectrophotometrically. The average drug content in each film was then calculated. The drug content is considered satisfactory if RES concentration was in the range of 85–115% of the theoretically stated amount according to USP National Formulary 24, 2000.

Film disintegration time
The 2x2 cm films were placed into the dissolution vessel containing 900ml of phosphate buffer (pH 6.8) which was maintained at 37±0.5°C with the paddle rotating at 100 rpm. The time required for complete disintegration of the film was determined visually. The experiment was conducted in triplicates and the data was presented as the mean ± standard deviation (Elagamy et al., 2019).

Fourier–transform infrared spectroscopy (FTIR)
The FTIR spectra of the prepared buccal films and their individual components were obtained to investigate possible interaction between RES and the film excipients. The disk preparation and scanning were as described for co-grinded mixtures (see above).

In vitro drug release
The dissolution studies were conducted according to previously published work with slight modification (Speer et al., 2019; Elagamy et al., 2019). USP dissolution equipment Type II (paddle method) was used employing 900 ml of 0.02 M phosphate buffer pH value of 6.8. The dissolution medium was equilibrated and maintained at 37 ± 0.5 °C with the paddle rotating at a rate of 50 rpm. Films containing amount equivalent to 20 mg of RES were chopped and placed in the dissolution vessels. Samples (5ml) were taken periodically, filtered and replaced with an equal volume of fresh medium. The drug content was then determined by UV spectrophotometry assay. The experiment was conducted in triplicate.

RESULTS AND DISCUSSION

Physical state characterization
To determine whether the changes of the crystalline state of RES during co-grinding process would occur or not, the physical state of unprocessed RES, co-formers and their formulations was investigated using different instrumental techniques.

Powder X-ray Diffraction (PXRD)
Powder X ray diffraction was conducted to study the crystalline structure of RES after co-processing with either AA or L-Ar. The diffractograms of the tested samples are shown in Figures 2. The characteristic 2theta (θ) values for each sample are presented in Table 3.

Table 3: The characteristic X-ray diffraction peaks of the pure resveratrol, ascorbic acid, arginine and different formulations.

2 Theta (degrees)	
RES	6.5, 13.1, 16.3, 19.1, 20.2, 22.2, 23.5, 25.1, 28.1,31.6, 41.9.
Processed RES (Positive control)	6.6, 16.2, 19.2, 22.2, 23.7, 28.2, 31.8, 36.2, 42.1.
Ascorbic acid	12.2, 18.3, 19.8, 19.9, 21.2, 22.6, 23.5, 24.5, 25.2 ,26.6, 30.1, 33.4, 34.4, 37.1, 37.8, 38.1, 38.4, 39.2 ,40.5, 41.2, 41.9, 43.2, 46.2, 46.9, 50.2, 53.5
Arginine	11.1, 14.8, 16.5, 19.2, 20.6, 22.9, 24.3, 27.5, 28.5, 29.7, 32.4, 35.9.
F1	11.9, 16.2, 18.1, 19.1, 19.8, 22.2, 23.5, 24.4,25.1, 26.7, 28.2, 30.1, 33.3, 36.2, 41.9.
F2	4.5, 12.1, 16.2, 18.2, 19.1, 19.8, 22.2, 23.6, 24.5, 26.7, 28.2, 30.1, 33.4, 42.2.
F3	10.4, 13.9, 16.1, 17.3, 19.1, 19.8, 22.3, 23.5,25.3, 27.9, 29.9, 35.6, 37.5, 41.5
F4	14.7, 16.1, 19.1, 22.1, 22.9, 27.4, 28.1.
F5	6.4, 14.8, 16.2, 19.1, 22.2, 23.0, 23.4, 27.5, 28.1, 29.7, 31.5.
F6	14.8, 19.2, 22.3, 23.0, 27.5.
PM1	12.1, 16.3, 17.2, 18.2, 19.1, 19.8, 19.8, 21.1, 22.2, 23. 5, 24.4, 25.3, 26.7, 27.7, 28.2, 30.3, 33.3, 34.3, 36.3, 37.1, 37.8, 39.1, 39.8, 40.3, 41.9, 42.7.

PM2	6.1, 9.2, 11.1, 13.2, 14.8, 16.2, 16.5, 17.3, 18.2, 19.1, 19.2, 20.2, 20.6, 21.5, 22.2, 23.0, 23.5, 24.3, 25.0, 27.5, 28.1, 28.5, 29.7, 31.4, 32.4, 33.5, 33.9, 35.9, 38.4, 39.1, 42.8, 45.7

PM1 and PM2 are the physically mixed mixtures of components of formulations F3 and F5, respectively.

PXRD spectra showed many intense diffraction peaks at 2θ values lies in the region from 6.2 to 31.2° for crystalline RES, from 12 to 46 ° for AA and from11.6 to 35.5 ° for L-Ar. These diffraction peaks and their intensities are in good correlation with the published data for RES, AA and L-Ar (Carletto et al., 2016; Palma-Rodríguez et al., 2018; Elkholy et al., 2020).

Positive control (wet grinded RES) showed minor alterations in the position of diffraction peaks with noticeable change in their intensities. This could reflect reduction in the particle size during the grinding process and possible conversion of the drug to the amorphous state (Essa et al., 2017).

The diffractogram of the co-grinded RES with AA (F1 (1:1) and F2 (1:2) RES: AA, respectively) showed a summation of the peaks of the two components of the mixture with reduced intensities (Figure 2A). Abolishment of some diffraction peaks was also noted (Table 2). These changes could be due to reduced particle size and/or possible transformation of the drug crystal lattice to the less ordered form (Bazeed et al., 2021). It is worth noting that at the higher molar ratio of AA (F3 (1:3)), new diffraction peaks were noticed at 2θ values of 10.37 °, 17.33 °, 35.59 ° and 41.48°. These new peaks are highlighted by arrows in Figure 2A. Appearance of these peaks would suggest the development of new crystalline species. Developing of new diffraction peaks were previously taken as indication of co-crystal formation and 1:3 ratio provided the optimum composition for this transformation (Essa et al., 2019; Arafa et al., 2021).

For RES co-grinded composite with L-Ar, the diffractograms showed a summation of peaks for both components with reduced intensities (Figure 2B). As mentioned earlier, the reduced peak intensities could be due to decreased RES crystalline structure or/and reduced particle size due to grinding. The absence of peaks of excess L-Ar at the higher molar ratio of 1:3 may suppose possible amorphousization of the excess amino acid (Elkholy et al., 2020).

The diffraction pattern of the physical mixtures for the selected formulations F3 (PM1) and F5 (PM2) are shown in Figure 2 and 2θ values are in Table 3. The recorded 2θ values are the summation of the those corresponding to the individual components. This indicates that there was no change in the crystalline structure of RES when physically mixed with the used additive.

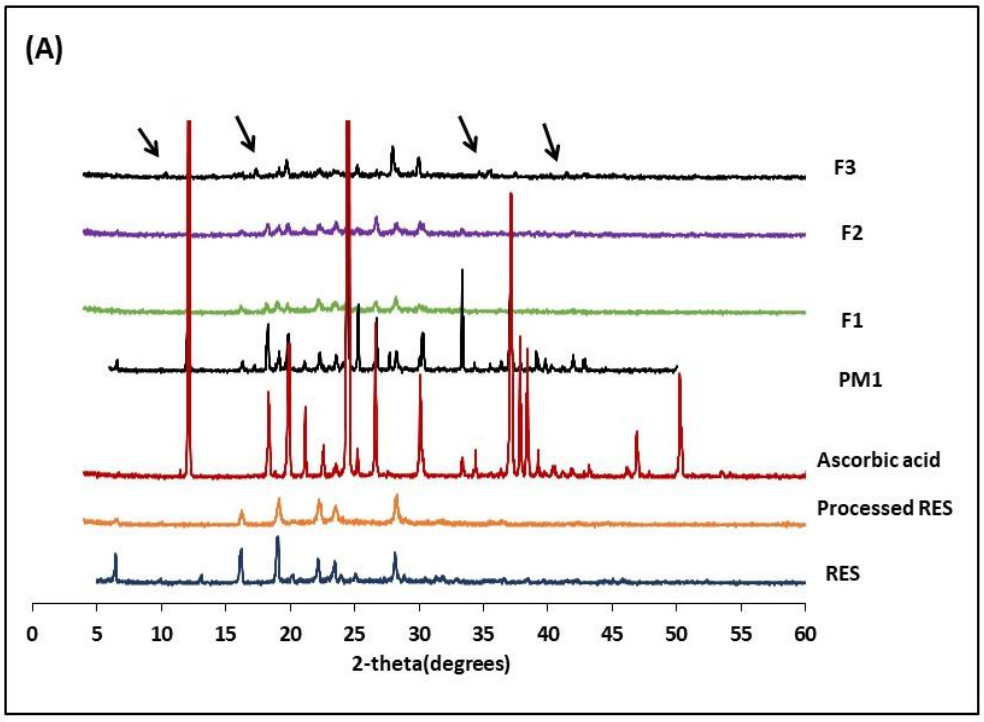

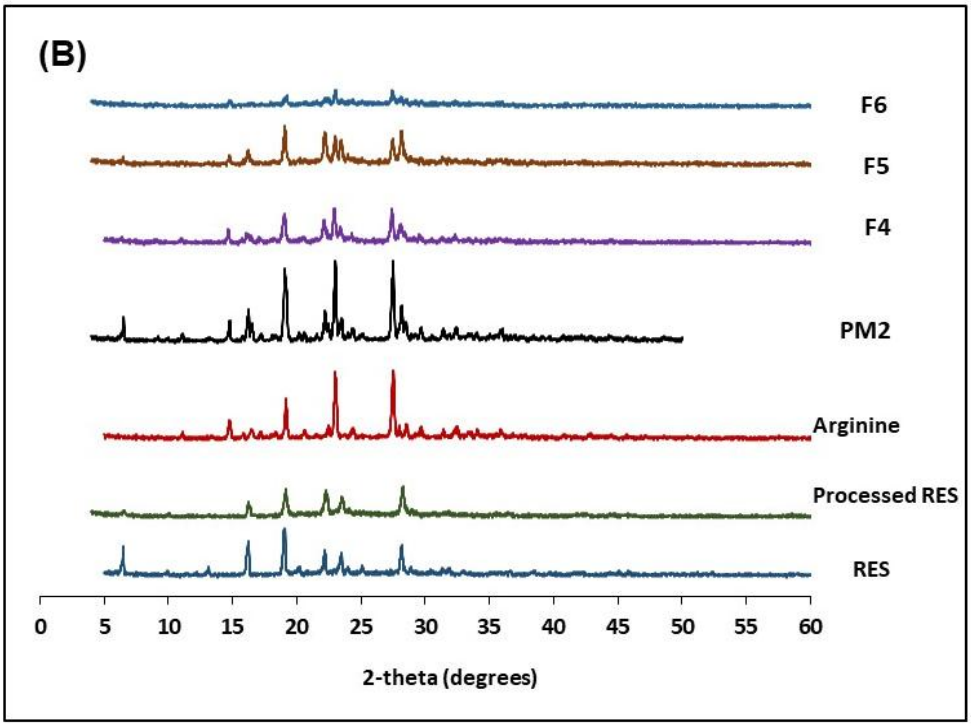

Figure 2: X-ray diffraction pattern of resveratrol (RES), processed RES, ascorbic acid (A), L-arginine (B) and different formulations. For Formulation details refer to Table I.

Fourier–transform infrared spectroscopy (FTIR)

FTIR for RES (raw and processed), AA, L-Ar and their co-processed composites are scanned from 4000 to 400 cm^{-1} and the results obtained are shown in Figure 3. FTIR spectrum of RES showed a typical trans olefinic band at 965.6 cm^{-1} and narrow band of O-H stretching vibration at 3227.3 cm^{-1} (Figure 3). The three intense bands at 1383.85, 1586.53 and 1590.21 cm^{-1} are corresponding to C–O stretching, C–C olefinic stretching and C–C aromatic double bond stretching, respectively. Processed RES (positive control) didn't show significant changes in peaks positions.

For AA, the absorption band at 1713 cm^{-1} is for stretching vibration of the carbonyl (C=O) group of the lactone ring. Band appearing at 1644 cm^{-1} is for C=C stretching vibration (Figure 3A). The spectrum also showed few peaks in the frequency range of 3225 through 3481 cm^{-1} corresponding to the different hydroxyl groups of the compound (Panicker et al., 2006).

FTIR spectrum of co-grinded RES and AA (formula F1 and F2) didn't reflect significant changes as the recorded spectra and can be considered as the summation of the spectra of both components (Figure 3A). The FTIR spectrum for formula F3 (1:3) showed significant alteration where the absorption band of carbonyl group of AA was broadened and shifted from 1713 cm^{-1} to lower wave number of 1652 cm^{-1}. The position of this shift is indicated by the arrow. The absorption band of OH group was also broadened. These changes are in consistent with the PXRD and confirm the interaction between RES and AA with the possible formation of new species. This new species could be, to a large extent, co-crystals and the molar ratio of 1:3 RES to AA is the stoichiometric ratio required for co-crystal formation.

The spectrum of L-Ar (Figure 3B) showed a broad absorption band of OH stretching in the range of 2440 to 3300 cm^{-1}. The primary amine stretching vibrations were noted at 3281 and 3525 cm^{-1}. The vibrational bands for C=O and N=O appeared at 1652 and 1620 cm^{-1}, respectively. Absorption bands appearing at 1311 and 1403 cm^{-1} are for bending vibrational changes of N-H and NH_2 groups, respectively. This spectrum with its characteristic vibrational bands for L-Ar is similar to published data (ElKholy et al., 2020; Shervington and Al-Tayyem 2001).

Co-processing RES with L-Ar didn't show significant changes in the spectra of formulations having low amino acid molar ratio (F4 and F5). Nevertheless, at the higher ratio of L-Ar (formula F6 1:3) there was a noticeable change. The major alteration was manifested as shift in the vibration band for C=O to a higher wavenumber of 1725 cm^{-1} (see the arow in Figure 3B). This indicates interaction between the two components with possible formation of more strong intermolecular bonds.

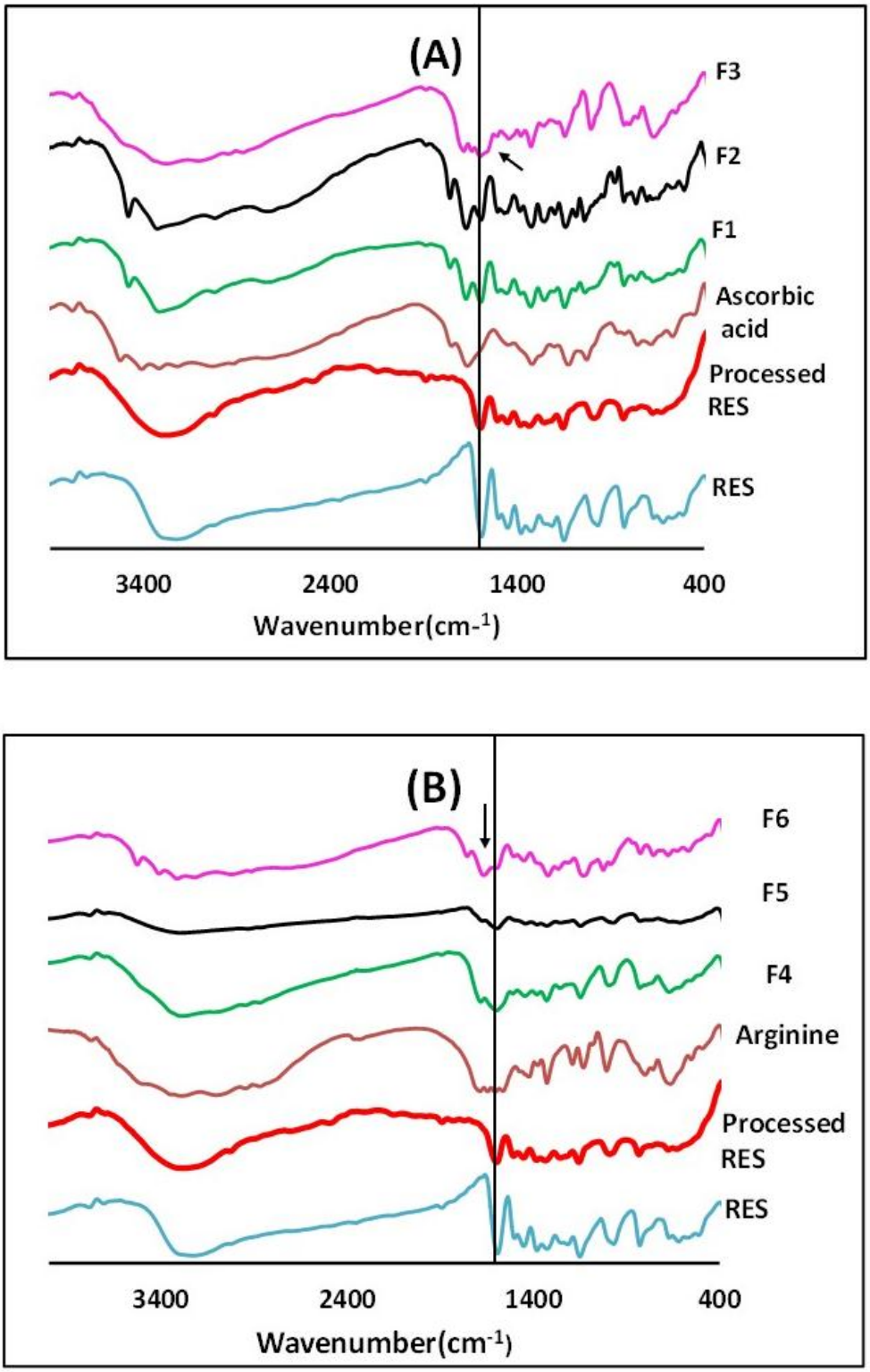

Figure 3: FTIR spectra of resveratrol (RES), processed RES, ascorbic acid (A), L-arginine (B) and their different formulations. For detailed formulations refer to Table I.

Differential Scanning Calorimetry

The thermal behavior of RES (raw and processed), AA, L-Ar, and their co-grinded composites are shown in Figure 4. The thermogram of pure RES showed sharp endothermic peak at Tm value of 269.6◦C (with enthalpy value of 200.8 J/g) corresponding to its melting and reflecting its crystalline nature. This thermal pattern agrees with reported thermogram for the same compound (Zhou et al., 2016). For wet grinded RES (positive control) there was no significant change in Tm or enthalpy compared to pure RES.

For AA the thermogram showed an endothermic peak at around 175.3^{o}C shortly followed by exothermic event recorded at 221.0^{o}C (Figure 4A). The first sharp endothermic peak is attributed to melting transition of the compound, while the exothermic peak could be due to the chemical degradation. This thermal pattern is like that reported by other investigators (Nicolov et al., 2019). The thermograms of co-processed RES and AA showed modulated thermal behavior compared to that of unprocessed RES, positive control and AA. The variation in the thermograms based on the relative proportion of RES to AA. At 1:1 (F1) and 1:2 (F2) RES:AA ratios, the endothermic peak of the drug disappeared with the appearance of two small broad peaks with a midpoint transition at 208◦C and 220◦C with decreased enthalpy recording 128 and 98.2 J/g, respectively. Meantime, the endothermic peak of AA was shifted to lower Tm of 166.9 and 168.5 ◦C for F1 and F2, respectively. Peak broadening and/or Tm shifting to a lower value were taken by other investigators as indication of reduced crystalline packing of the compound (Bettinetti et al., 2002). There is a considerable chance that some RES dissolved in ethanol during the co-grinding steps that later precipitated, after ethanol evaporation, as fine crystals of weaker intermolecular interaction. Increasing AA concentration (F3), its melting transition started to be broader and more shifted to slightly higher Tm of 171.5◦C compared to the other two formulations. Meantime, the peak of RES disappeared with the appearance of new peak as a fused shoulder following AA peak. The Tm of the new peak was detected at 190◦C with enthalpy of 214 J/g. This may suggest formation of new species with slightly higher intermolecular force (Figure 4A). The thermogram for physical mixture PM1 showed a slight shift in AA peak with the disappearance of drug peak. This unexpected behavior suggests that on heating up the physical mixture in DSC, RES progressively interacts with and dissolve in AA which melts at lower temperature. Similar finding and suggestion were recorded (Vippagunta et al., 2002; El Maghraby and Alomrani, 2009). This assumption is supported by the proved drug crystalline structure by the PXRD results.

The thermogram of L-Ar showed three thermal events appeared at 88.5, 222.7 and 234.3^{o} C (Figure 4B). The first broad peak could be attributed to evaporation of adsorbed water, the second peak is due to melting and the third one is for decomposition. This thermal behavior coincides with the reported thermogram by other published data (Elkholy et al., 2020; Zhang et al., 2014). Co-grinding of RES with L-Ar at different molar ratios produced thermal transitions that differ from those of their individual components. L-Ar melting transition was decreased to 162, 159 and 162◦C for F4, F5 and F6, respectively. Meantime, thermal event of RES showed significant peak broadening with reduced Tm compared to the pure RES. The melting transition for F4, F5 and F6 were detected as broad peaks with Tm of 201, 220 and 202◦C, respectively. The enthalpy similarly decreased giving values of 79, 93 and 72 (J/g) in the same order. This may indicate reduced crystalline packing structure of the prepared co-grind mixtures.

The thermogram of physical mixture PM2 showed thermal patterns that may indicate possible interaction between L-Ar and RES during the heating process. This was reflected by shifted endothermic peak of L-Ar to about 173ºC and disappearance of RES endotherm. The later could be explained similar to PM1.

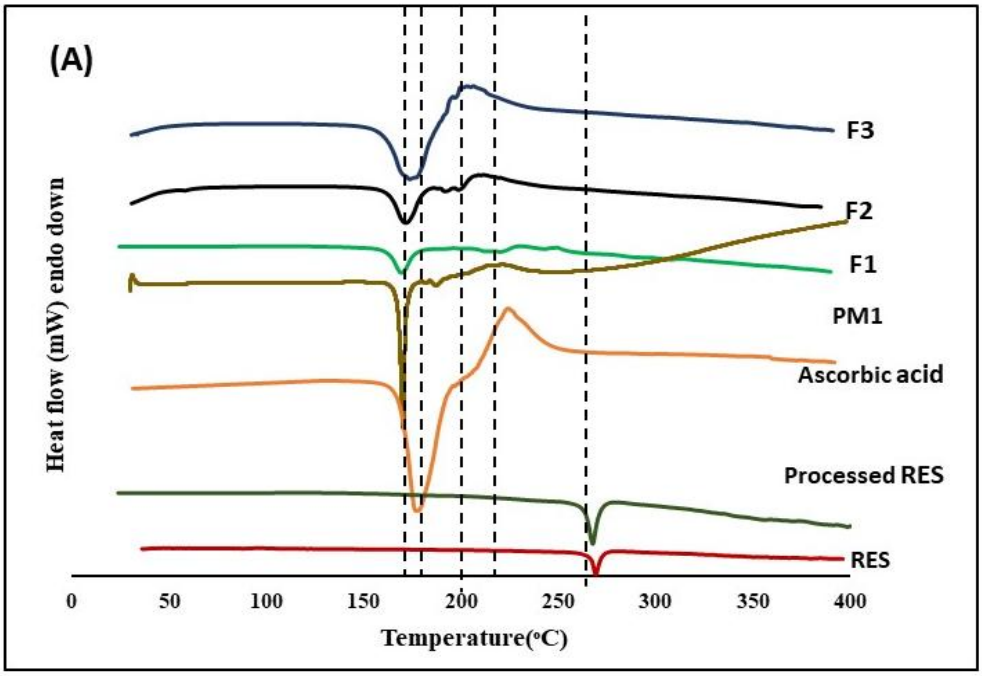

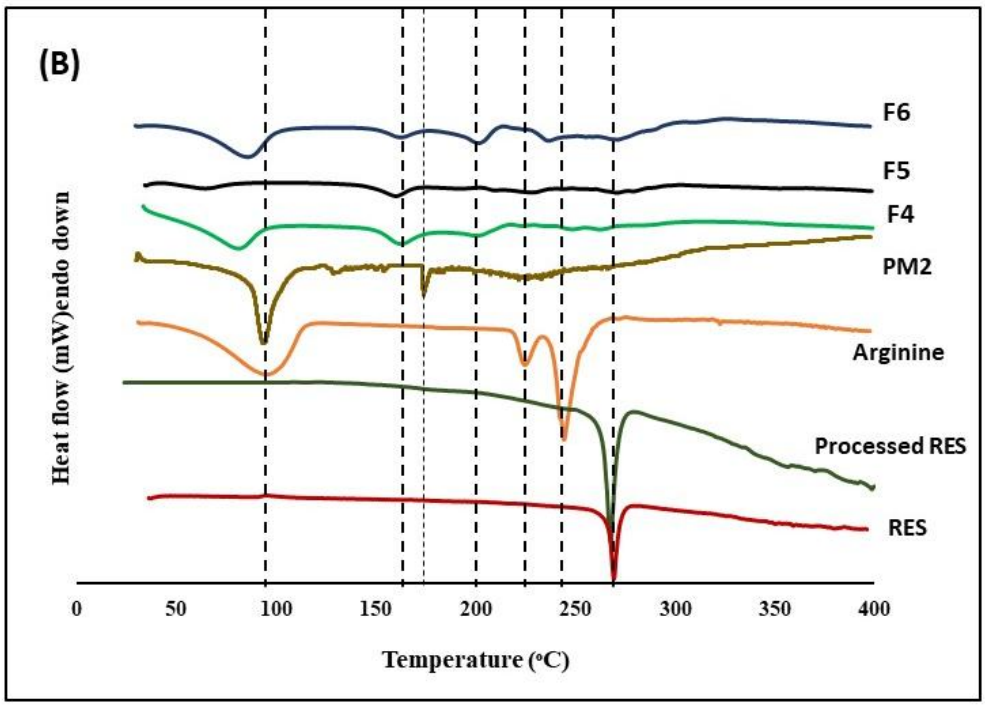

Figure 4: DSC thermograms of resveratrol (RES), processed RES, ascorbic acid (A), L-arginine (B) and their different formulations. For detailed formulations refer to Table I.

In vitro dissolution studies

Dissolution studies were performed to monitor the effect of co-processing of RES with AA or L-Ar on the dissolution rate. Figure 5 shows the dissolution profiles of RES from its unprocessed, processed (positive control) and different formulations. To compare between different formulations, dissolution parameters were computed from the dissolution data and presented in Table 4 as percentage drug released after 5 minutes (Q5) and dissolution efficiency (%DE).

Additionally, similarity factor was employed to compare between different formulations using the following equation:

$$\boldsymbol{F2}=50\times\log\left\{\left[1+\frac{1}{n}\sum_{t-1}^{n}(Rt-Tt)^2\right]^{-5}\right\}\times 100$$

Where *F*2 represents the similarity factor, n is the number of data points, *Rt* is the percentage amount dissolved from reference at time t, and *Tt* is the percentage amount dissolved from the test sample at the same time. *F*2 values higher than 50 reflects similarity of the two dissolution profiles (Kour et al.,2015).

The dissolution profile of RES showed a slow release with only 23% of the loaded dose liberated after 5 minutes. This together with a limited dissolution efficiency of 30% reflects the hydrophobic nature of RES. This result is in good correlation with previously published data for RES (Balata et al., 2016). Ethanol assisted grinding of RES in absence of additives (positive control) showed a similar dissolution parameter to the unprocessed one (P > 0.05, using student *t*-test) indicating that kneading of drug alone was not enough to improve dissolution. Similarity factor more than 50 confirms this supposition.

For RES and AA composites (Figure 5A), there were a significant increase in RES dissolution compared to both processed and unprocessed ones (P<0.05). Formula F1 (1:1) and F2 (1:2) liberated about 32 and 34% of the loaded dose after 5 minutes, respectively (***F2*** value >50). However, the dissolution efficiency was higher from F2 (Table 4). This improvement in RES dissolution could be due to particle size reduction, with subsequent increment in surface area, as indicated by PXRD. Another possible reason could be the reduced RES crystallinity, due to the co-grinding conditions, as supposed by DSC. Increasing AA content to 1:3 (F3) significantly (P < 0.05) improved dissolution parameters that was superior to F1 and F2. Similarity factor of less than 50 proves such superiority. The obtained high-RES dissolution after processing with AA could be due to many interrelated factors such: possible hydrogen bond formation, as reflected from FTIR data; particle size reduction, reduced drug crystallinity, in addition to possible formation of new species, most probably co-crystals, as indicated by PXRD. Therefore, formula F3 was taken as the optimum formula for RES and AA combination.

RES and L-Ar composite improved dissolution RES, with the improvement depended on the relative proportions of the amino acid to RES (Figure 5B; Table 1). Formulations F4, increased RES dissolution with a prompt release of 60.3 % after 5 minutes with dissolution efficiency of 76.3. Increasing L-Ar concentration to 1:2 (F5) improved further RES release compared to F1

(Similarity factor ***F1*** of <50). The same justifications for the improved RES from AA-containing formulations can be applied here. Unexpectedly, increasing L-Ar concentration to 1:3 (F6) showed dissolution behavior that is significantly lower than that for F4 and F5 as indicated by similarity factor values more than 50. This finding is against the well accepted conception of increasing co-former stoichiometric concentration should further increase API dissolution. This unexpected reduced dissolution may be also attributed to the generation of supersaturated RES dissolution layer around each particle resulting in its precipitation. Similar finding was obtained by other investigators and was similarly interpreted (Li and Matzger, 2016). For this reason, F5 was selected as the optimum formula showing the highest RES dissolution when co-grinded with L-Ar.

For comparative purposing, dissolution of physically mixed components of formula F3 and F5 (PM1 and PM2, respectively) were investigated. The dissolution profiles are in Figure 5 and dissolution parameters are in Table 4. The dissolution parameters were significantly ($P < 0.05$) lower than that from the corresponding co-grinded mixtures with DE of 30.4% and 38.9% for PM1 and PM2, respectively. This proves the need for co-grinding technique in enhancing RES dissolution.

Table 4: The dissolution parameters of resveratrol from different formulations and pure form.

Formula	Q5%	DE (%)
Pure resveratrol	24.3±0.5	29.7± 1.1
F1	32.5±2.5	58.8± 1.1
F2	34.1±0.9	68.3± 3.2
F3	45.9±1.1	75.0± 2.8
F4	60.4 ± 8.5	76.3 ±2.3
F5	74.8 ±6.7	82.9±1.4
F6	54.7±3.5	66.1±0.7
PM1	36.2±2.6	30.4±0.4
PM2	38.1±0.5	38.9±0.3

- Q5 amount of resveratrol dissolved after 5 minutes
- DE is dissolution efficiency expressed as percentage

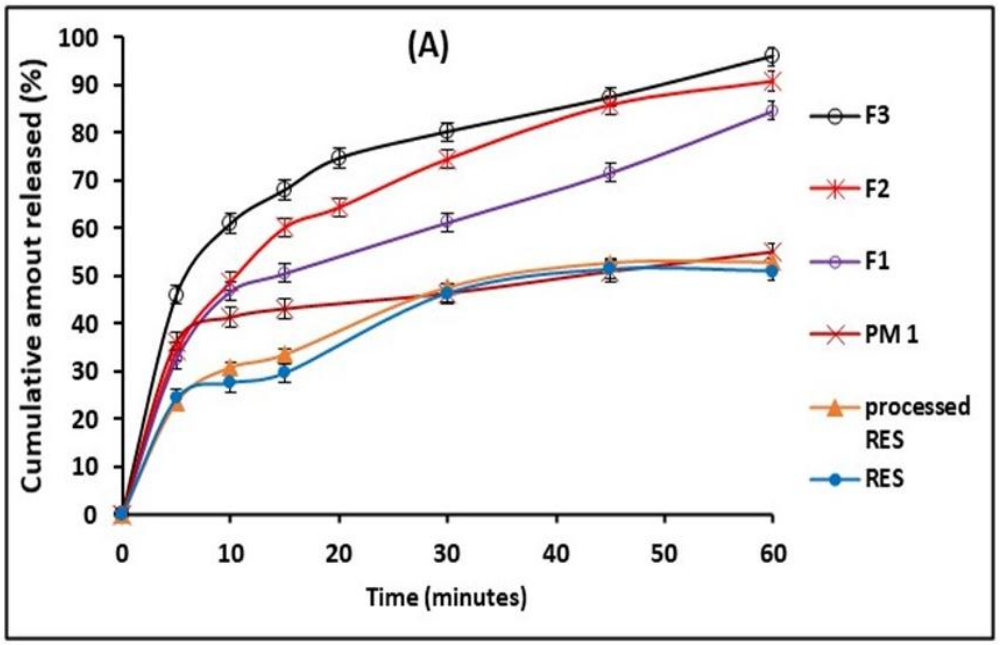

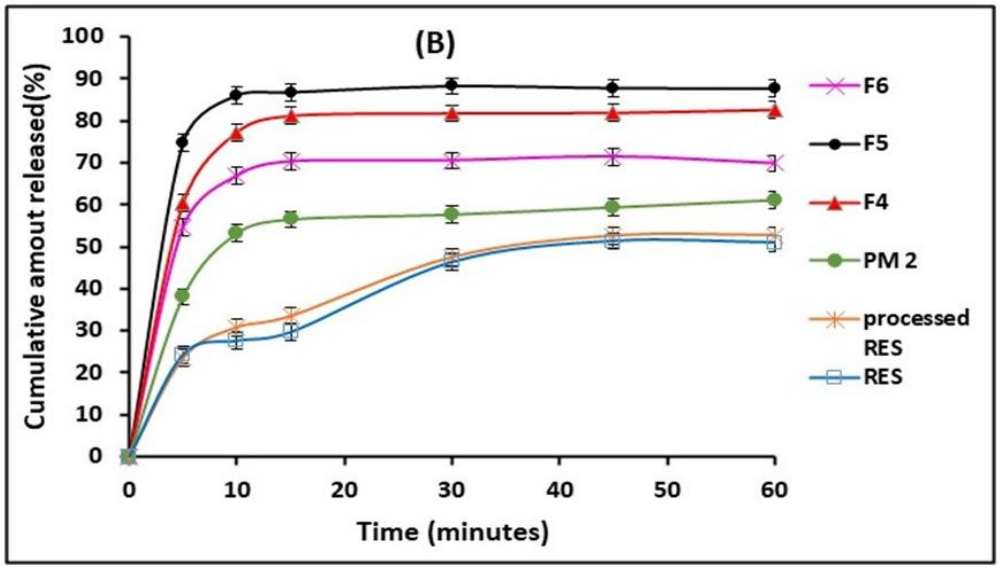

Figure 5: In vitro dissolution of resveratrol from different formulations prepared using ascorbic acid (A) or L-arginine (B). Formulation details are presented in Table 1.

Anti-oxidant activity

This test was conducted to ensure that RES retains its free radical scavenging activity after co-processing. The adopted method is an accepted method for determining the antioxidant activity (AOA) of many compounds from natural source. The violet color of DPPH solution is reduced to a yellow-colored product that is measured calorimetrically. The optimized formulations (F3 and F5), that showed better dissolution parameters, were evaluated along with unprocessed RES. The percentage AOA against DPPH radical versus concentration of the used samples are shown in Figure 6. RES alone showed its hydrogen donating ability to scavenge free radical. This ability was retained after processing with either AA or L-Ar as there was no noticeable reduction in the free radical scavenging ability of RES in the tested formulations. Therefore, wet co-grinding of RES with either excipient preserved the antioxidant potential of RES in the newly formed crystalline species (Nicolov et al., 2019). The IC50 values (the amount of antioxidant material required to scavenge 50% of DPPH initial concentration) were calculated. The IC50 values were 10.5±0.57, 7.8±0.3 and 17.7±2.4 µg/ml for unprocessed RES, Formula F3 and Formula F5, respectively, relative to 11.0±0.6 µg/ml for the reference. Based on these values, the antioxidant activity of F3 is stronger than that of F5. This may be explained by the augmented effect between RES and AA in F3.

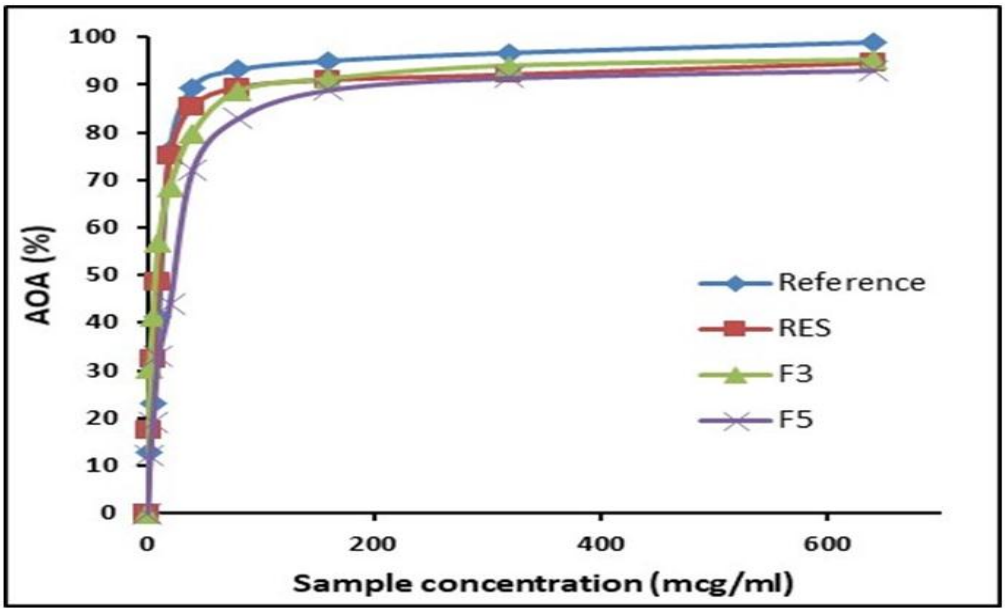

Figure 6: Antioxidant activity of resveratrol (RES) and co-grinded mixtures of RES with either ascorbic acid (F3) or L-arginine (F5). Reference sample represents pure ascorbic acid. Standard error bars were omitted for clarity.

Evaluation of the buccal films

The prepared films were evaluated for weight, thickness, folding endurance, surface pH value, drug content and the time required for complete dissolution. The results are presented in Table 2. Films were transparent with weight uniformity and homogenous film thickness. The pH value ranged from 5.7 to 6.4. This indicates the suitability of the films for buccal mucosa with no expected irritation. Buccal films with similar pH values have been reported (Elagamy et al., 2019; Kapetanovic et al., 2011). The drug content ranged from 92 to 102%. reflecting good uniformity of drug within the films (Table 2).

As there is no standardized official guidelines or specifications for oral dispersible film, it was stated that disintegration time requirements for oral dispersible tablets, that vary between 30 s and 3 min, can be applied to oral dispersible films (European Pharmacopeia Commission, Tablets, 2013). Therefore, all films were acceptable as they underwent rapid disintegration within 45–72 seconds. Comparable values have been reported for buccal films by other researchers (Elagamy et al., 2019; Maher and Salem, 2016; Venkateswarlu, 2016). The longer time taken by Film 1 containing unprocessed API (75 sec) could be due to the hydrophobicity of RES that slightly affected film wettability compared to the other two films. For folding endurances, all films were flexible and showed minor scratches after 300 folding. This indicates that the type and concentration of the plasticizer were suitable for the intended use.

Fourier–transform infrared spectroscopy (FTIR)

The FTIR spectra for pure RES, HPMC, PVP and buccal films prepared using the optimized co-grinded mixture using AA (Film2), L-Ar (Film3) as well as pure RES (Film1) are shown in Figure 7A.

The FTIR spectrum of pure PVP showed strong absorption band for carbonyl group at a frequency of 1623 cm^{-1}. Another broad band was detected at the range of 2986 to 3680 cm^{-1} due to water adsorption. Another band at 2888 cm^{-1} is due to CH stretching. This spectrum correlates well with published data (El Maghraby et al., 2014). For HPMC, the spectrum showed the characteristic broad band in the range of 2900–3669 cm^{-1} for hydroxyl groups, and broad band at 980 cm^{-1} due to pyranose ring. This spectrum is in good correlation with the published spectra for the same polymer (El Maghraby et al., 2014; Elagamy et al., 2019). RES showed its characteristic peaks described as before.

Regarding spectra for the prepared films, bands due to C–O stretching, C–C olefinic stretching and C–C aromatic double bond stretching of RES were broaden indicating hydrogen bond formation. The characteristic C=O band for PVP was slightly broaden with decreased intensity. Additionally, a small shoulder appeared at slightly higher wave number. This could indicate possible hydrogen bonding between PVP and other components. Similar findings were recorded and similarly explained (Elagamy et al., 2019).

In vitro drug dissolution of buccal films

The *in vitro* drug dissolution profiles from the prepared films are shown in Figure 7B as a relation between cumulative amount permeated as function of time. The dissolution parameters are shown in Table 2. Incorporation of unprocessed RES in the control film (Film1) resulted in the liberation of 52% of the loaded drug in the first 5 minutes followed by slow drug dissolution pattern. The dissolution efficiency was 40% (Table 2). Such relatively high initial dissolution compared to the unprocessed drug can be attributed to the presence of RES in a very minute crystals in the thin film. This resulted in a massive increment in the surface area with subsequent increased dissolution. Hydrogen bond formation could be another contributing factor for such enhancement. However, this dissolution still does not fulfill the requirements for buccal dosage forms or even immediate release oral medications. Incorporation of treated RES with either AA (Film 2) or L-Ar (Film3) markedly increased dissolution rate. Both film2 and film3 recorded Q5 of 89.0 and 80.0%, respectively ($P< 0.05$). The dissolution efficiency was similarly increased. This is because co-processing of RES with either AA or L-Ar enhanced the dissolution rate by co-amorphousization and/or formation of new species with more aqueous solubility compared to the parent compound.

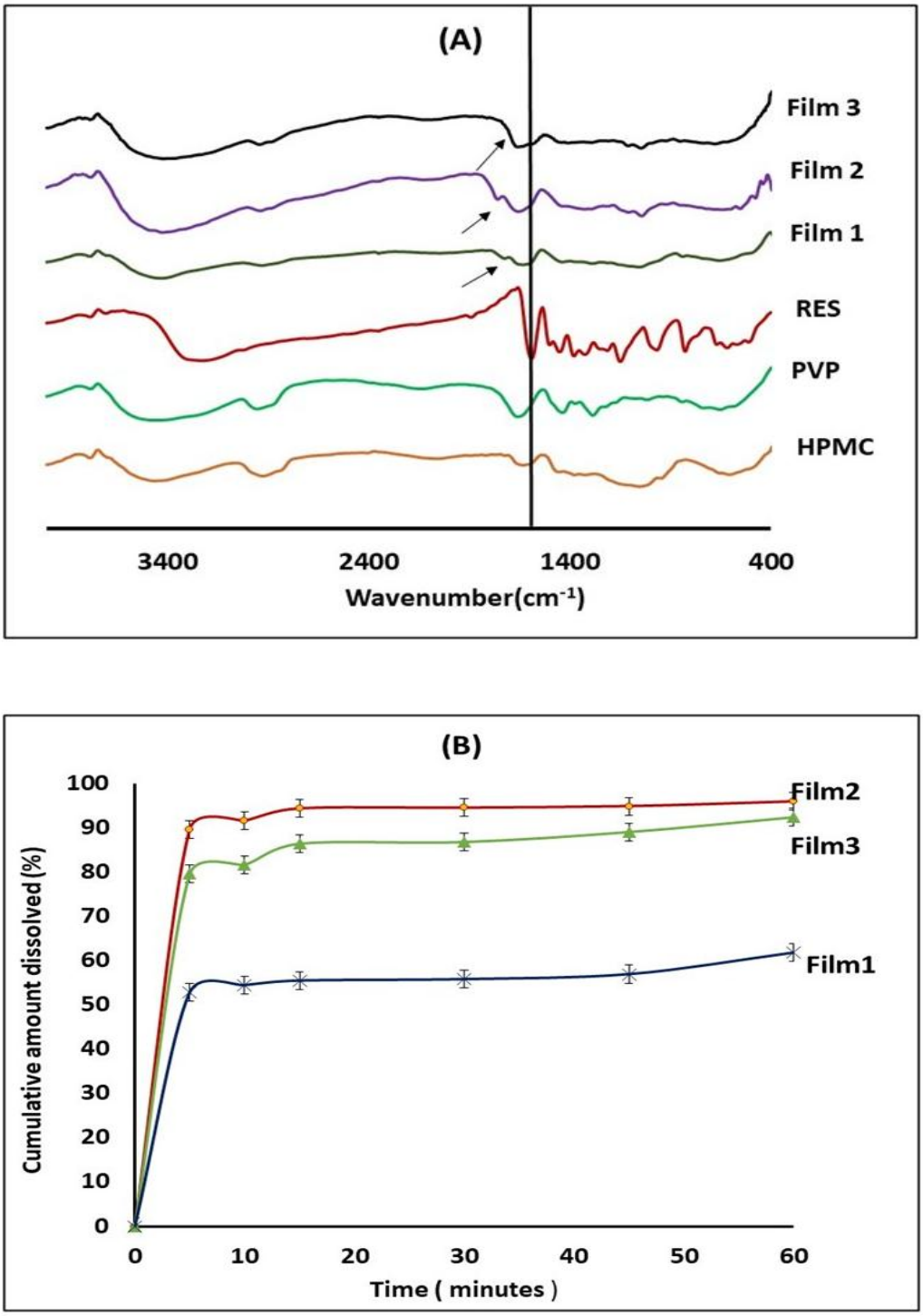

Figure 7: (A) FTIR spectra of unprocessed resveratrol (RES), polyvinylpyrrolidone (PVP), hydroxypropylmethylcellulose (HPMC) and buccal films; (B) *in vitro* dissolution of RES from different buccal films. Detailed films compositions are presented in Table 2.

CONCLUSION

Ascorbic acid and L-arginine, as guest molecules, significantly improved resveratrol's dissolution. Modulation of the crystalline nature of RES was evidenced by physical characterization, that also suggested possible formation of new species. The prepared composites reserved the antioxidant activity of resveratrol. The optimized formulations were successively formulated into fast dissolving buccal films. The rapid release of RES in the buccal cavity is expected to improve the bioavailability via pre-gastric absorption that would reduce its exposure to pre-systemic degradation by metabolizing enzymes.

Disclosure statement

No potential conflict of interest was reported by the authors.

REFERENCES

1. Abu-Serie M.M., El-Gamal B.A., El-Kersh M.A. et al. Investigation into the antioxidant role of arginine in the treatment and the protection for intralipid-induced non-alcoholic steatohepatitis. Lipids Health Dis., 2015; 14: 128. https://doi.org/10.1186/s12944-015-0124.
2. Arafa M.F, Alshaikh R.A, Abdelquader M.M, et al. Co-processing of Atorvastatin and Ezetimibe for Enhanced Dissolution Rate: In Vitro and In Vivo Correlation, AAPS PharmSciTech, 2021; 22: 59.
3. Attia M, Essa E. A, Zaki R.M, et al.An Overview of the Antioxidant Effects of AscorbicAcid and Alpha Lipoic Acid (in Liposomal Forms) as Adjuvant in Cancer Treatment, Antioxidants, 2020; 9: 359.
4. Balata G.F, Essa E.A, Shamardl H.A, et al. Self-emulsifying drug delivery systems as a tool to improve solubility and bioavailability of resveratrol. Drug Des Devel Ther, 2016; 10: 117-28.
5. Bettinetti GP, Sorrenti M, Rossi S, et al. Assessment of solidstate interactions of naproxen with amorphous cyclodextrin derivatives by DSC. J Pharm Biomed Anal, 2002; 30: 1173–1179.
6. Brindle L, Krochta J. Physical properties of whey protein hydroxypropyl methylcellulose blend edible films. J Food Sci., 2008; 73: 446–454.
7. Carletto B, Berton J, Ferreira T.M, et al. Resveratrol-loaded nanocapsules inhibit murine melanoma tumor growth, Colloids Surf. B., 2016; 144: 65–72.
8. Chi Z., Wang M., Yang L., et al. Fourier transform near-infrared spectroscopy used for purity determination of rhein-L-arginine cocrystal (argirein). Anal. Sci., 2013; 29: 661–664.
9. Elagamy HI, Essa E.A, Nouh A et al. Development and evaluation of rapidly dissolving buccal films of naftopidil: in vitro and in vivo evaluation, Drug Dev Ind Pharm, 2019; 45: 1695-1706.
10. Elkholy N. E, Sultan A. A, Elosaily G.H, et al. Acetone assisted co-processing of meloxicam with amino acids for enhanced dissolution rate, Pharm Dev Technol., 2020; 25(7): 882-891.
11. El Maghraby G.M. and Alomrani A.H. Synergistic Enhancement of Itraconazole Dissolution by Ternary System Formation with Pluronic F68 and Hydroxypropyl methylcellulose. Sci Pharm, 2009; 77; 401–417.
12. El Maghraby GM, Elsergany RN. Fast disintegrating tablets of nisoldipine for intra-oral administration. Pharm Dev Technol, 2014; 19: 641–650.
13. Essa EA, Elmarakby A, El Maghraby G, et al. Controlled precipitation for enhanced dissolution rate of flurbiprofen: Development of rapidly disintegrating tablets. Drug Dev. Ind. Pharm, 2017; 24: 1-10
14. Essa E. A, Elbasuony A. R, Abdelaziz E. A, et al. Co-crystallization for enhanced dissolution rate of bicalutamide: Preparation and evaluation of rapidly disintegrating tablets. Drug Dev Ind Pharm, 2019; 45(8): 1215-1223.
15. Ha ES, Sim WY, Lee SK, et al. Preparation and Evaluation of Resveratrol-Loaded Composite Nanoparticles Using a Supercritical Fluid Technology for Enhanced Oral and Skin Delivery. Antioxidants, 2019; 8(11): 554. doi:10.3390/antiox8110554.
16. Ha ES, Choi DH, Baek IH, et al. Enhanced Oral Bioavailability of Resveratrol by Using Neutralized Eudragit E Solid Dispersion Prepared via Spray Drying. Antioxidants (Basel), 2021; 10(1): 90. doi:10.3390/antiox10010090.
17. Hao J, Gao Y, Zhao J, et al. Preparation and optimization of resveratrol nanosuspensions by antisolvent precipitation using Box-Behnken design. AAPS PharmSciTech, 2015; 16(1): 118-128. doi:10.1208/s12249-014-0211-y.
18. Kapetanovic IM, Muzzio M, Huang Z, et al. Pharmacokinetics, oral bioavailability, and metabolic profile of resveratrol and its dimethylether analog, pterostilbene, in rats. Cancer Chemother Pharmacol, 2011; 68(3): 593-601. doi:10.1007/s00280-010-1525-4.
19. Karagianni A, Malamatari M, Kachrimanis K. Pharmaceutical cocrystals: new solid phase modification approaches for formulation of APIs. Pharmaceutics, 2018; 10(1): 18–32.
20. Kour P, Kataria MK, Bilandi A. Dissolution rate enhancement of pioglitazone by solid dispersion technique. IAJPR, 2015; 5(07): 2664-81.
21. Kovac-Besović E. E., Duric K., Kalodera, Z., et al. Identification and isolation of pharmacologically active triterpenes in betuale cortex, betula pendula roth., Betulaceae. Bosn. J. Basic Med. Sci., 2009; 9(1): 31–38. doi: 10.17305/bjbms.2009.2853.
22. Kristl J, Teskac K, Caddeo C, et al. Improvement of cellular stress response on Resveratrol in liposomes. Eur J Pharm Biopharm, 2009; 73(2): 253–259.
23. Khan K. The concept of dissolution efficiency. J Pharm Pharmacol, 1975; 27: 48–49.
24. Li Z, Matzger AJ. Influence of Coformer Stoichiometric Ratio on Pharmaceutical Cocrystal Dissolution: Three Cocrystals of Carbamazepine/4-Aminobenzoic Acid. Mol. Pharmaceutics, 2016; 13(3): 990–995.
25. Maher M, Ali M, Salem H, et al. In vitro/in vivo evaluation of an optimized fast dissolving oral film containing olanzapine coamorphous dispersion with selected carboxylic acids. Drug Deliv, 2016; 23(8): 3088–3100.
26. Marques F.Z., Markus M.A., Morris B.J. Resveratrol: Cellular actions of a potent natural chemical that confers a diversity of health benefits. *Int. J. Biochem. Cell Biol.*, 2009; 41: 2125–2128. doi: 10.1016/j.biocel.2009.06.003.

27. Meepripruk, M., Bumee, R., Somphon, W., et al. Crystal growth and physical characterization of acyclovir crystallized with ascorbic acid and zinc chloride. J. Life Sci. Technol, 2016; 4: 56–59. doi: 10.18178/jolst.4.2.56-59.
28. Naeem D, Osman M, El Maghraby G, et al. Salt and non-salt forming excipients to improve the dissolution of dexibuprofen; formulation of chewable tablets. EJBPS, 2020; 7(1): I-I I.
29. Nasr M, Almawash S, Bazeed A.Y, et al.Bioavailability and Antidiabetic Activity of Gliclazide-Loaded Cubosomal Nanoparticles , Pharmaceuticals, 2021; 14(8): 786.
30. Nicolov M, Ghiulai RM, Voicu M, et al. Cocrystal Formation of Betulinic Acid and Ascorbic Acid: Synthesis, Physico-Chemical Assessment, Antioxidant, and Antiproliferative Activity. Front Chem, 2019; 7: 92. Published 2019 Feb 21. doi:10.3389/fchem.2019.00092.
31. Panicker C.Y, Varghese H.T, Philip D, FT-IR, FT-Raman and SERS spectra of Vitamin C, Spectrochimica Acta Part A, 2006; 65: 802–804.
32. Rahman M.M., Islam M.B., Biswas M. et al. In vitro antioxidant and free radical scavenging activity of different parts of Tabebuia pallida growing in Bangladesh. BMC Res Notes, 2015; 8: 621.
33. Risuleo G. Chapter 33—Resveratrol: Multiple activities on the biological functionality of the cell. In: Gupta R.C., editor. *Nutraceuticals*. Academic Press; Boston, MA, USA, 2016; 453–464.
34. Rodríguez H.MP, Ramírez JA, Torres AV, using modified starch/maltodextrin microparticles for enhancing the shelf life of ascorbic acid by the spray-drying method, Starch, 2018; 70: 7-8.
35. Ryman S.G, El Shaikh A.A, Shaff N.A, et al. Proactive and reactive cognitive control rely on flexible use of the ventrolateral prefrontal cortex, Hum Brain Mapp, 2018; 40(3): 955-966.
36. Shan L, Wang B, Gao G, et al. L-Arginine supplementation improves antioxidant defenses through L-arginine/nitric oxide pathways in exercised rats. J Appl Physiol, 1985; 115(8): 1146-55.
37. Shervington A, Al-Tayyem R. Arginine. In: H.G. Brittian, editor. Analytical profiles of drug substances and excipients, vol.27. New York: Academic Press, 2001; 1–32.
38. Shimoda H, Taniguchi K, Nishimura M, et al. Preparation of a fast-dissolving oral thin film containing dexamethasone: possible application to antiemesis during cancer chemotherapy. Eur J Pharm Biopharm, 2009; 73: 361–365.
39. Smith A.J, Kavuru P, Wojtas L, et al. Cocrystals of Quercetin with Improved Solubility and Oral Bioavailability, Mol. Pharmaceutics, 2011; 8: 1867–1876.
40. Speer I, Preis M, Breitkreutz J. Dissolution testing of oral film preparations: Experimental comparison of compendial and non-compendial methods, Int. J. Pharm., 2019; 561: 124-134.
41. United States Pharmacopeia National Formulary 24. Rockville (MD): United States Pharmacopeial Convention, 2000.
42. Venkateswarlu K. Preparation and evaluation of fast dissolving buccal thin films of bufotenin. J ln Silici In Vitro Pharmacol, 2016; 103: 179–191.
43. Vippagunta S.R., Maul K.A., Tallavajhala S., Grant D.J.W. Solid-state characterization of nifedipine solid dispersions. Int J Pharm, 2002; 236: 111–123.
44. Weyna D.R, Cheney M.L, Shan N, et al. Improving solubility and pharmacokinetics of meloxicam via multiple-component crystal formation. Mol.Pharm, 2012; 9(7): 2094–2102.
45. Yen, G.C. and Duh, P.D. Scavenging effect of methanolic extracts of peanut hulls on free radical and active oxygen species, J Agric Food Chem, 1994; 42: 629-632.
46. Zhang L, Wu C, Gu T, et al. Preparation, characterization and cytotoxic activity of rhein argininate, Anal. Methods, 2014; 6: 3838-3841.
47. Zhou Z, Li1 W, Sun W, et al. Resveratrol Cocrystals with Enhanced Solubility and Tabletability, Int J Pharm, 2016; 509(1-2): 391-399.